

## **Supporting information:**

### **Effect of Interaction among Magnesium Ions, Anion and Solvent on Kinetics of Magnesium Deposition Process**

*Feilure Tuinxun,<sup>a</sup> Kentaro Yamamoto,<sup>a\*</sup> Toshihiko Mandai,<sup>b</sup> Yoshitaka Tateyama,<sup>b</sup> Koji Nakanishi,<sup>a</sup> Tomoki Uchiyama,<sup>a</sup> Toshiki Watanabe,<sup>a</sup> Yusuke Tamenori,<sup>c</sup> Kiyoshi Kanamura,<sup>d</sup> Yoshiharu Uchimoto<sup>a</sup>,*

<sup>a</sup>Graduate School of Human and Environmental Studies, Kyoto University, Sakyo-ku, Kyoto 606-8501, Japan

<sup>b</sup>Center for Green Research on Energy and Environmental Materials and International Center for Materials Nanoarchitectonics, National Institute for Materials Science (NIMS), Tsukuba, Ibaraki 305-0044, Japan

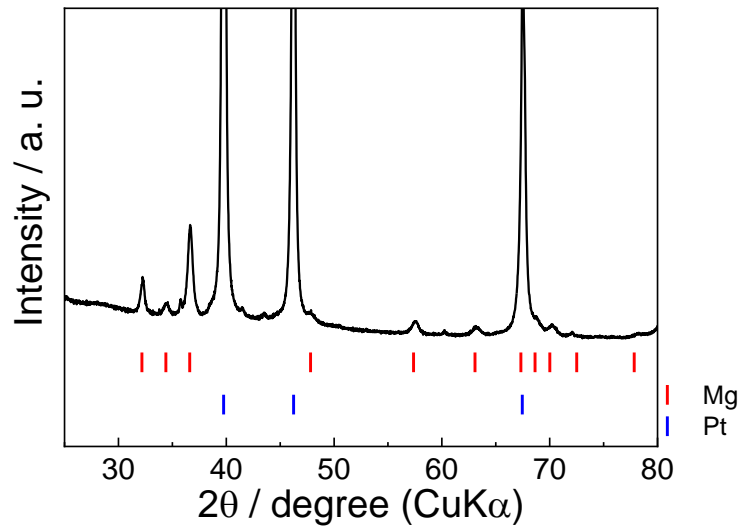
<sup>c</sup>Research & Utilization Division, Japan Synchrotron Radiation Research Institute (JASRI), Sayo, Hyogo 679-5198, Japan

<sup>d</sup>Department of Applied Chemistry, Graduate School of Urban Environmental Sciences, Tokyo Metropolitan University 1-1 Minami-Ohsawa, Hachioji, Tokyo 192-0397, Japan

Corresponding author

\*E-mail: yamamoto.kentaro.4e@kyoto-u.ac.jp

(a)



(b)

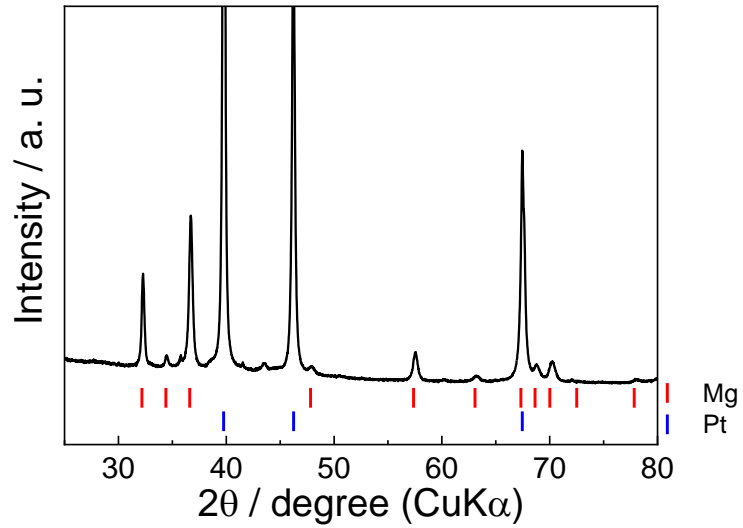
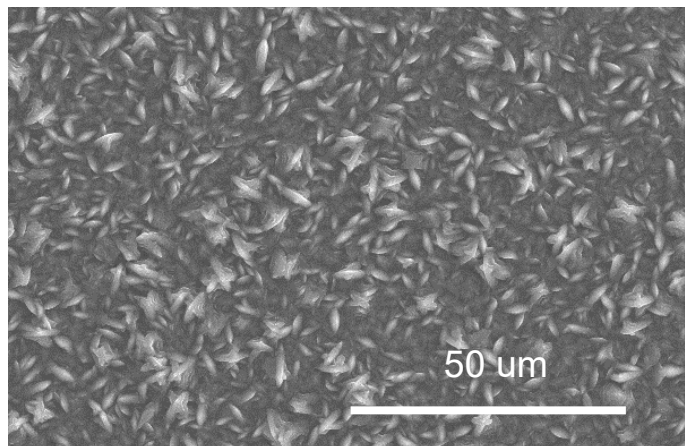


**Figure S1.** XRD patterns of electrodeposited of (a) 0.3 M  $Mg[B(HFIP)_4]_2$ /triglyme (b) 0.3 M  $Mg[B(HFIP)_4]_2$ /2-MeTHF on Pt substrate.

(a)



(b)

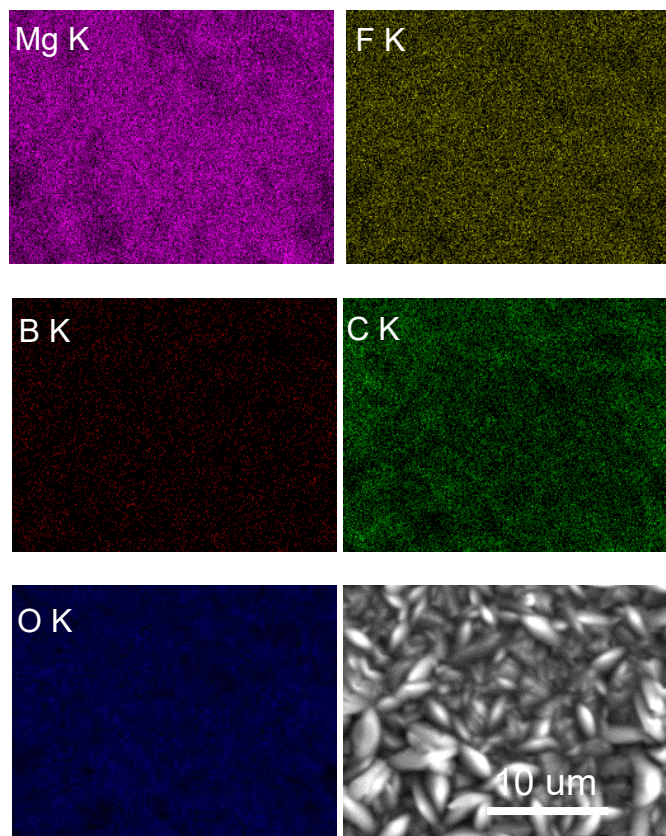


**Figure S2.** (a) SEM image, (b) EDX mapping and spectrum of Pt substrate after electrochemical measurements in 0.3 M  $\text{Mg}[\text{B}(\text{HFIP})_4]_2$ /triglyme.

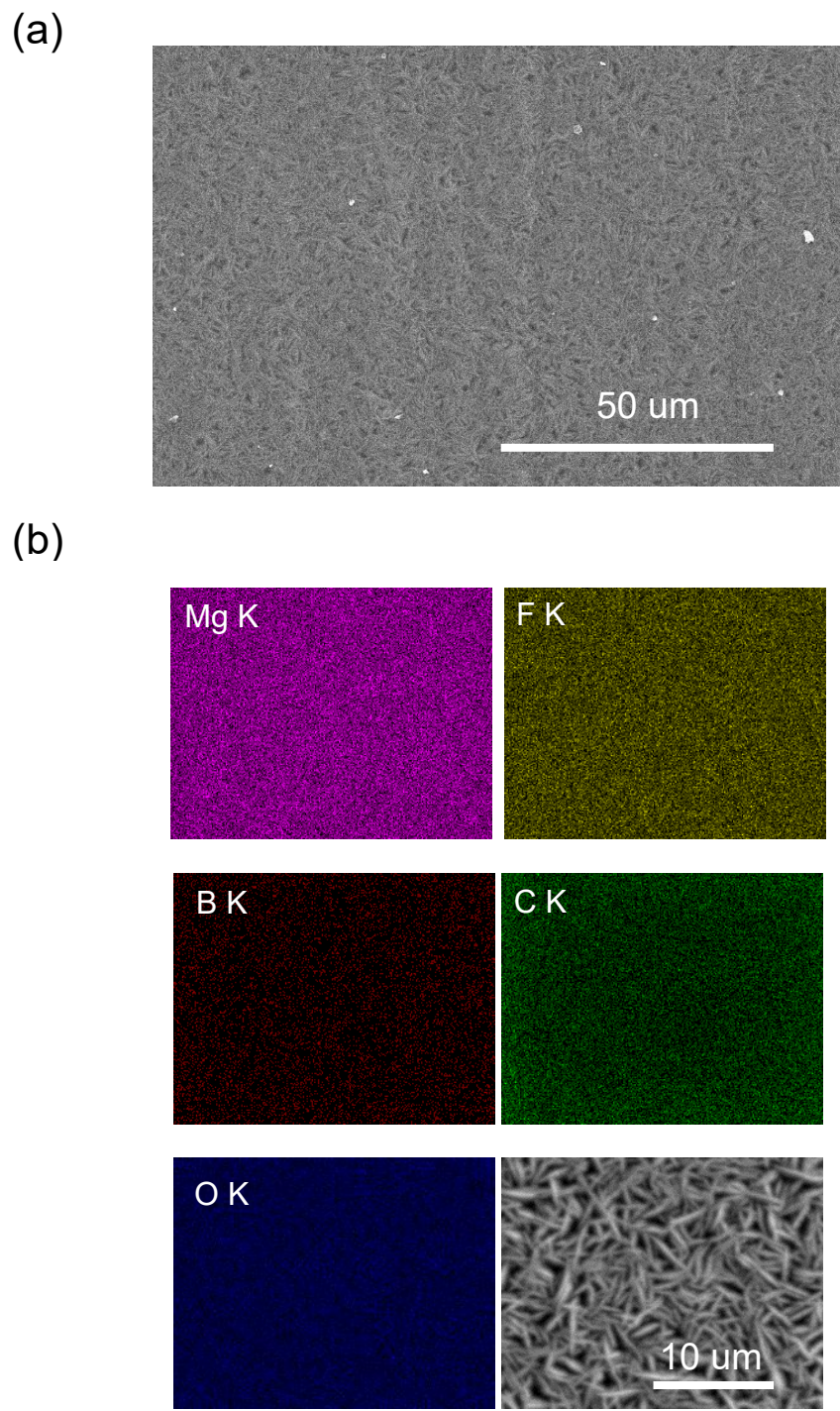
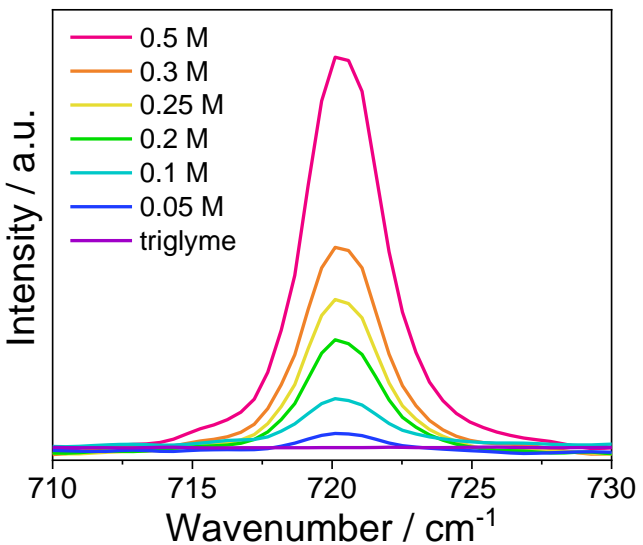


**Figure S3.** (a) SEM image, (b) EDX mapping and spectrum of Pt substrate after electrochemical measurements in 0.3 M  $\text{Mg}[\text{B}(\text{HFIP})_4]_2$ /2-MeTHF.

(a)



(b)

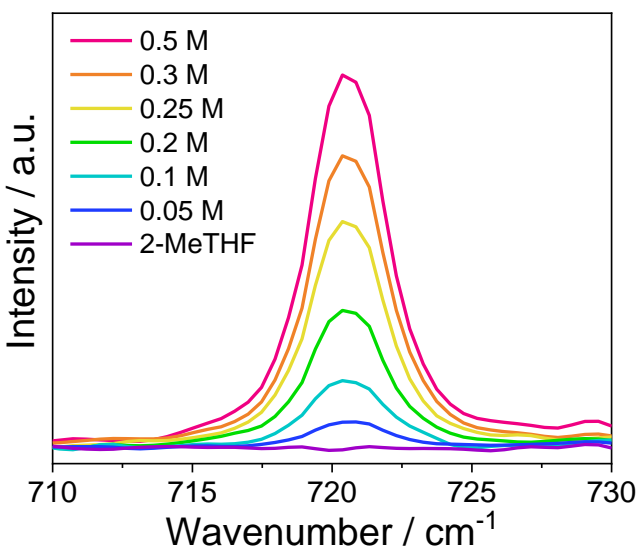


**Figure S4.** Raman spectra of (a)  $\text{Mg}[\text{B}(\text{HFIP})_4]_2$ /triglyme and (b)  $\text{Mg}[\text{B}(\text{HFIP})_4]_2$ /2-MeTHF with several concentrations in the region between 710 and 730  $\text{cm}^{-1}$

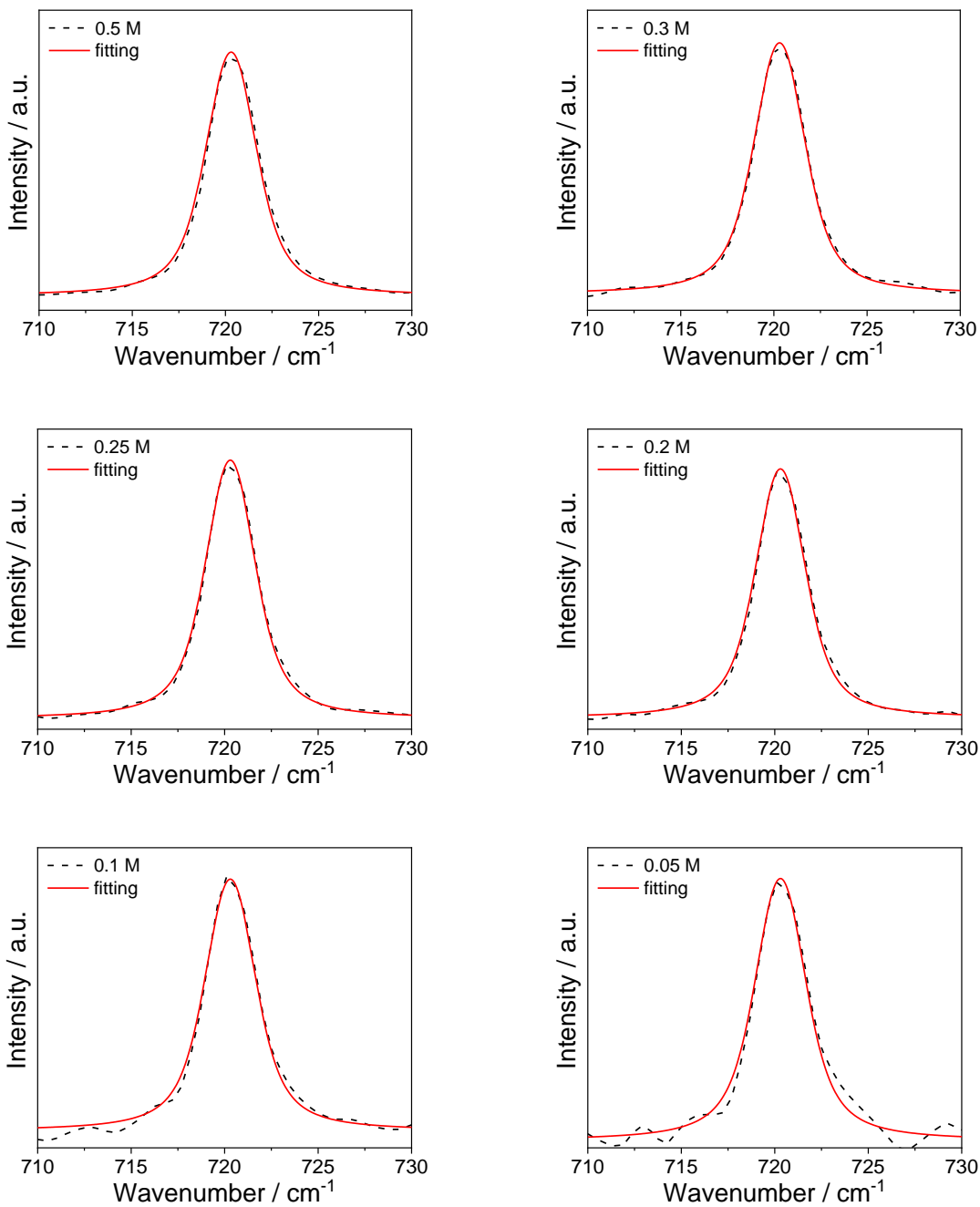


**Figure S5.** Raman spectra and voigt function fitting results of  $\text{Mg}[\text{B}(\text{HFIP})_4]_2/\text{triglyme}$  in several concentrations in the wave number between 710 and 730 cm<sup>-1</sup>.

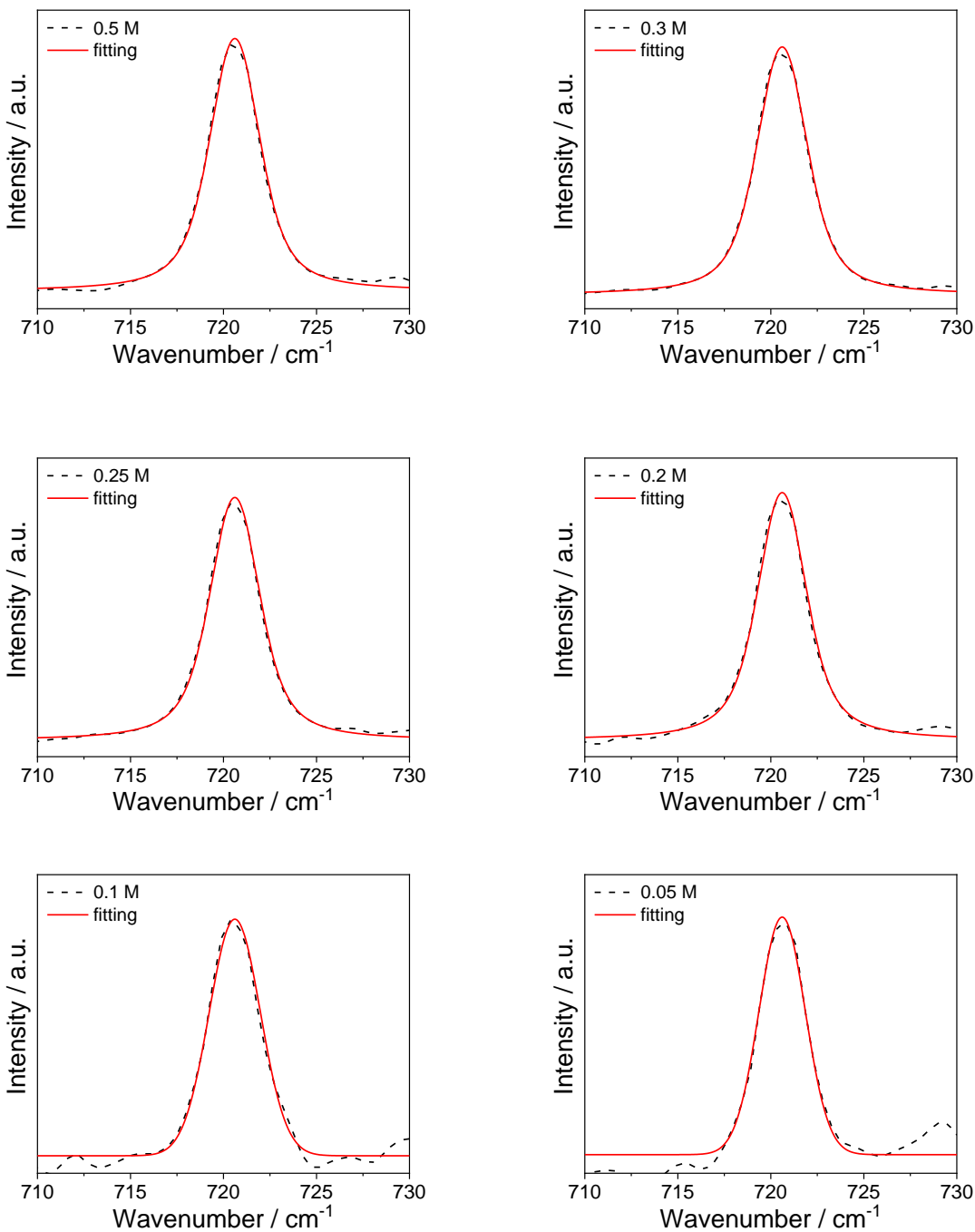
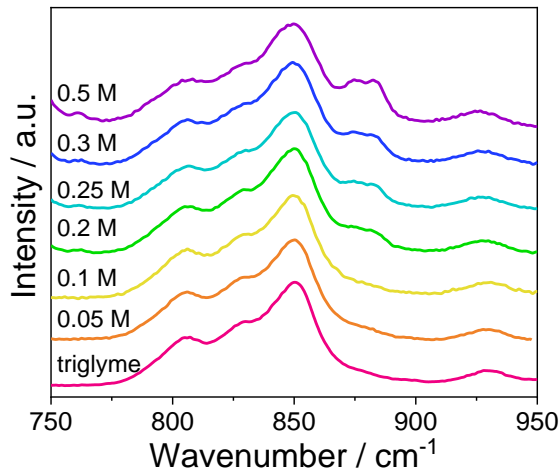
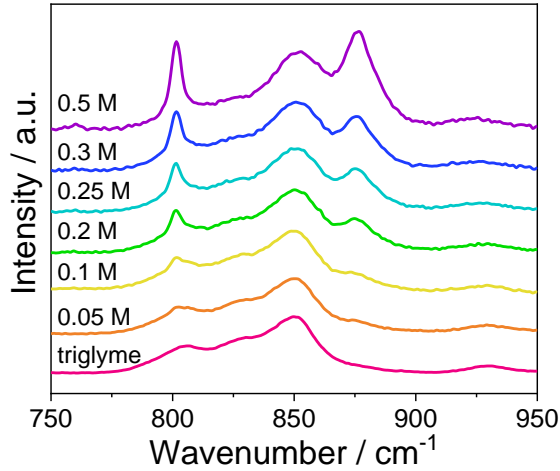


**Figure S6.** Raman spectra and Voigt function fitting results of  $\text{Mg}[\text{B}(\text{HFIP})_4]_2/2\text{-MeTHF}$  in several concentrations in the wave number between 710 and 730 cm<sup>-1</sup>.

(a)



(b)



(c)

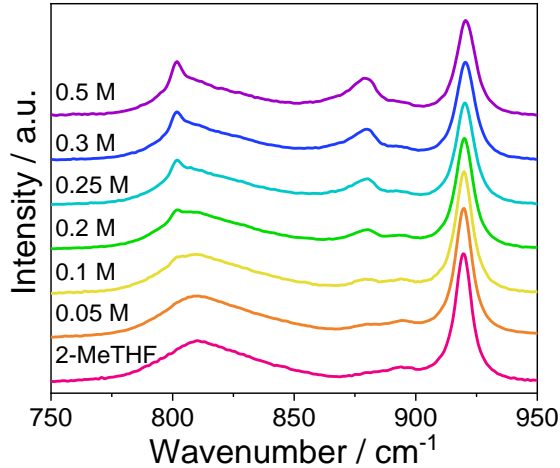


**Figure S7.** Raman spectra of (a) Mg[TFSA]<sub>2</sub>/ triglyme (b) Mg[B(HFIP)<sub>4</sub>]<sub>2</sub>/triglyme and (c) Mg[B(HFIP)<sub>4</sub>]<sub>2</sub>/2-MeTHF in the wave number between 750 and 950 cm<sup>-1</sup>.

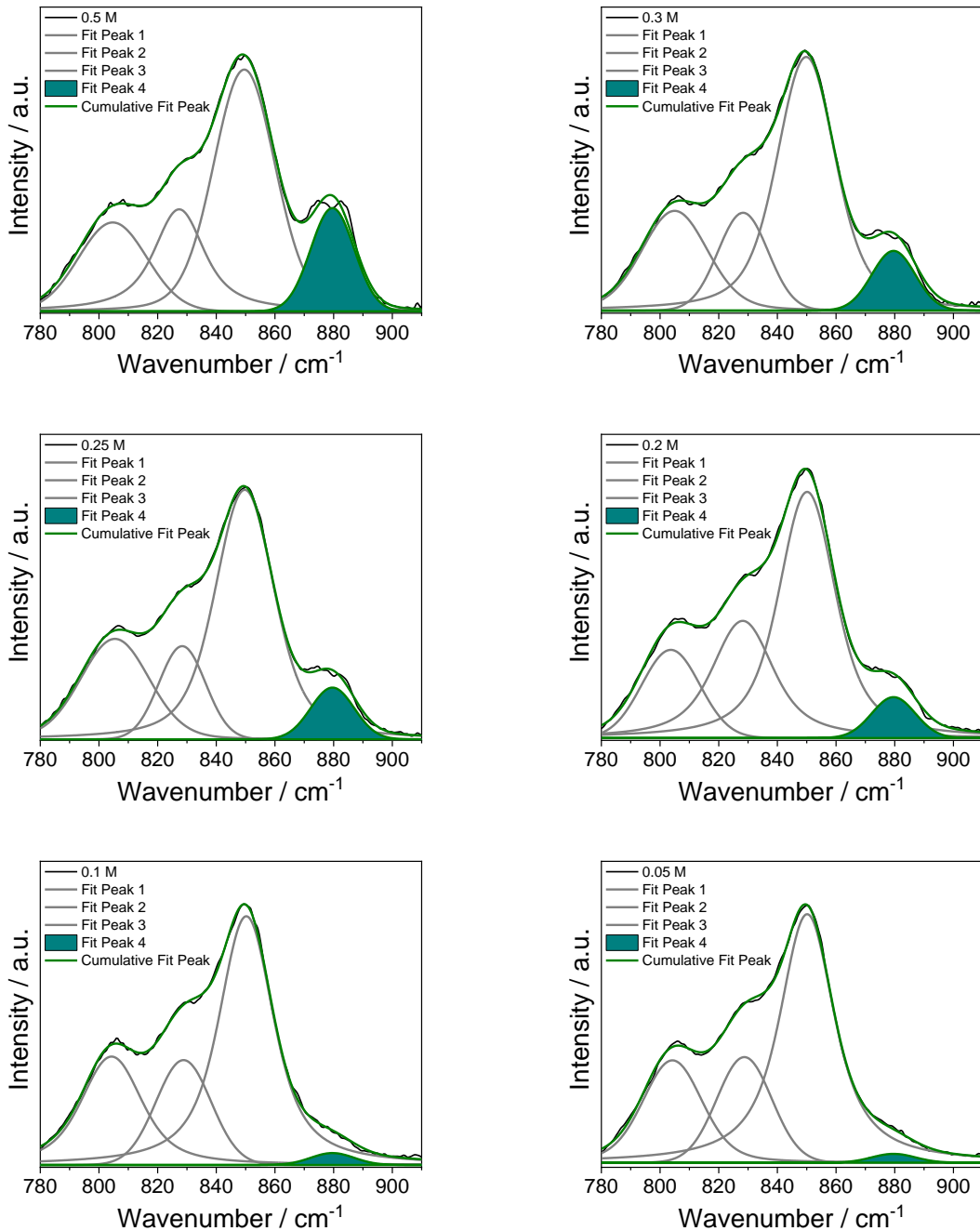


**Figure S8.** Raman spectra and Voigt function fitting results of  $\text{Mg}(\text{TFSA})_2/\text{triglyme}$  in several concentrations in the wave number between  $780$  and  $910\text{ cm}^{-1}$ .

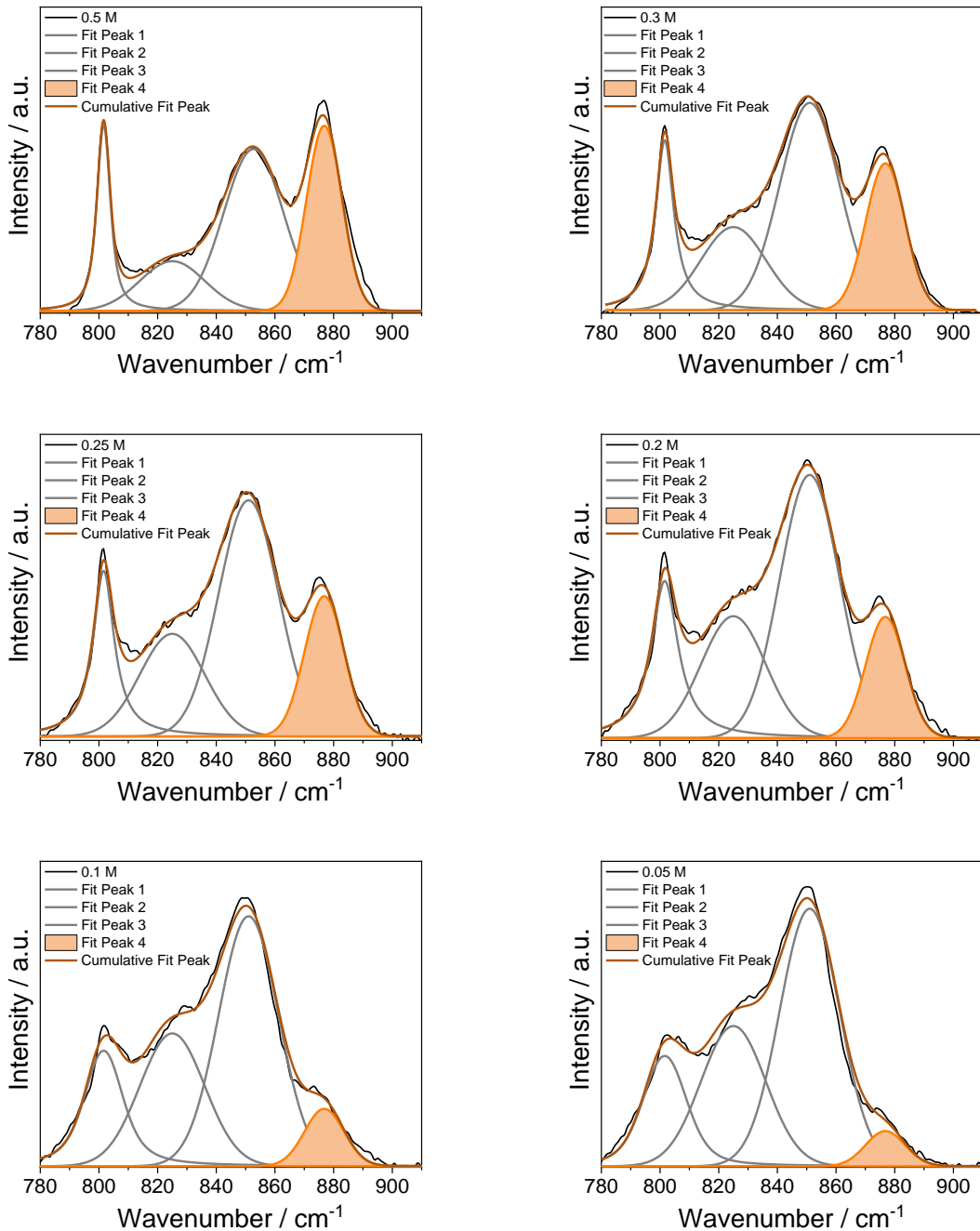


**Figure S9.** Raman spectra and Voigt function fitting results of  $\text{Mg}[\text{B}(\text{HFIP})_4]_2$ /triglyme in several concentrations in the wave number between 780 and 910  $\text{cm}^{-1}$ .

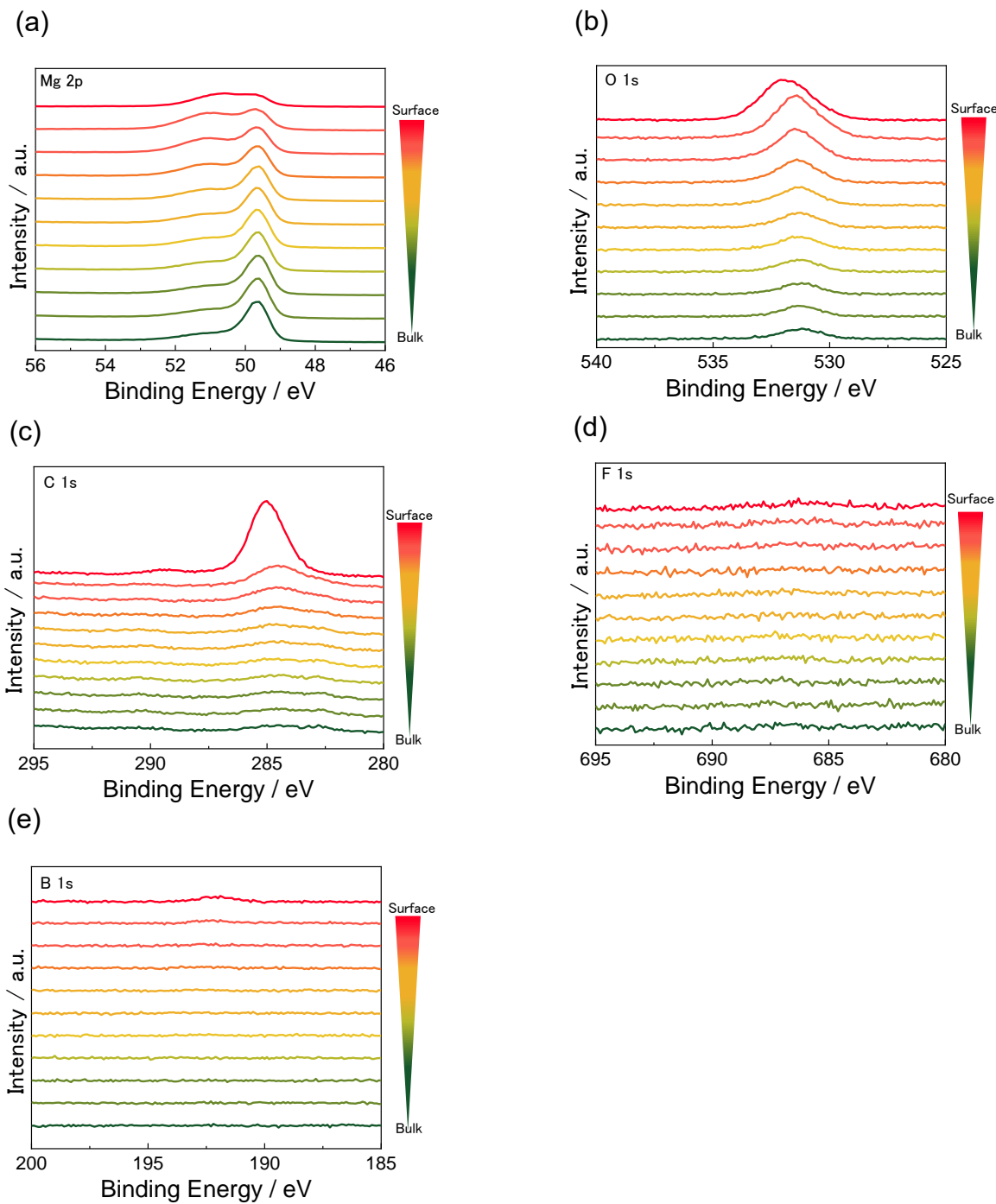


**Figure S10.** XPS spectra for the deposited magnesium metal on platinum substrate by using immersed in the 0.3 M  $\text{Mg}[\text{B}(\text{HFIP})_4]_2$ /triglyme; (a) Mg 2p, (b) O 1s, (c) C 1s, (d) F 1s and (e) B 1s. The Ar ion beam sputtering times are marked at the right side of the graph.

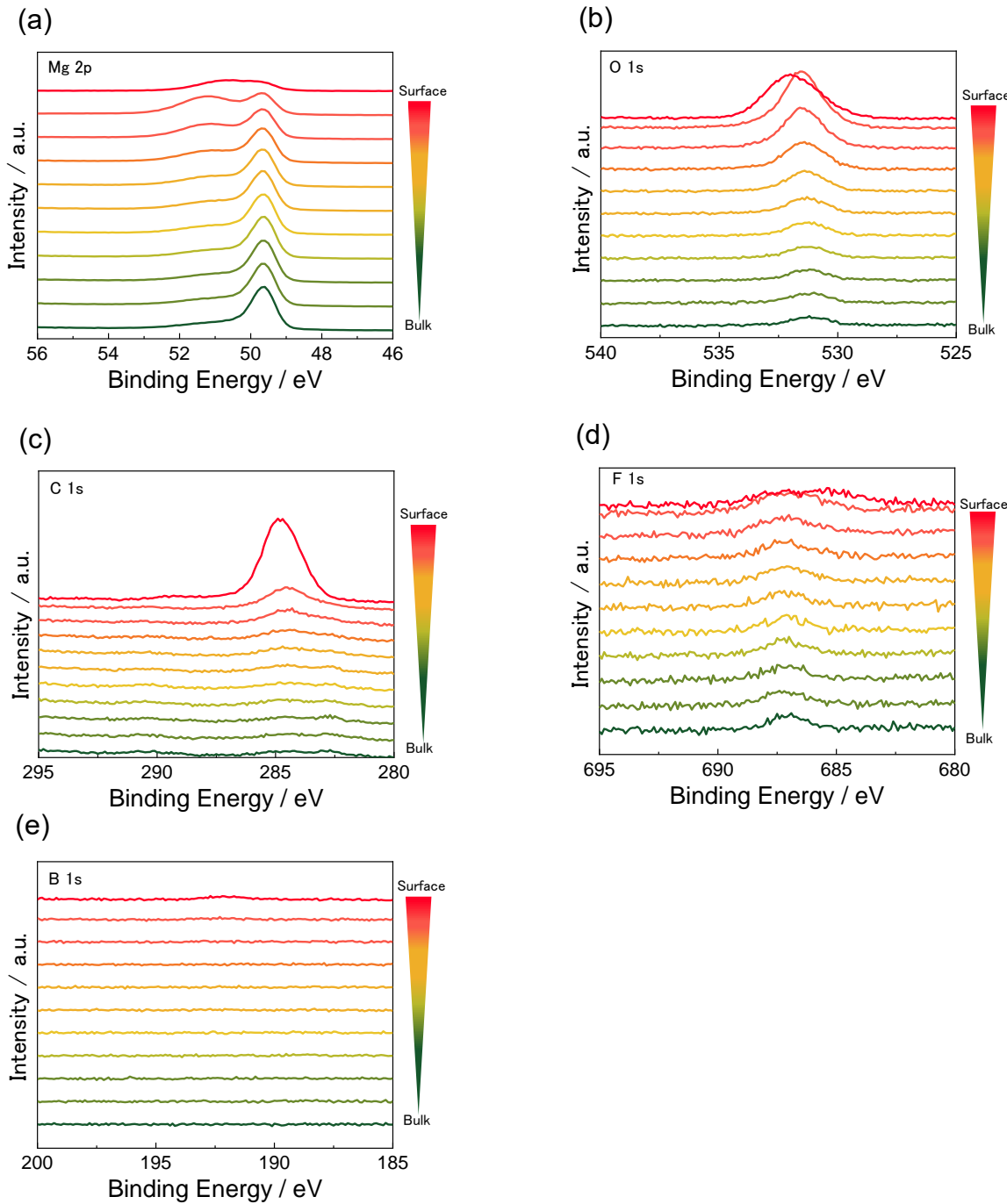


**Figure S11.** XPS spectra for the deposited magnesium metal on platinum substrate by using immersed in the 0.3 M  $\text{Mg}[\text{B}(\text{HFIP})_4]_2$ /2-MeTHF; (a) Mg 2p, (b) O 1s, (c) C 1s, (d) F 1s and (e) B 1s. The Ar ion beam sputtering times are marked at the right side of the graph.

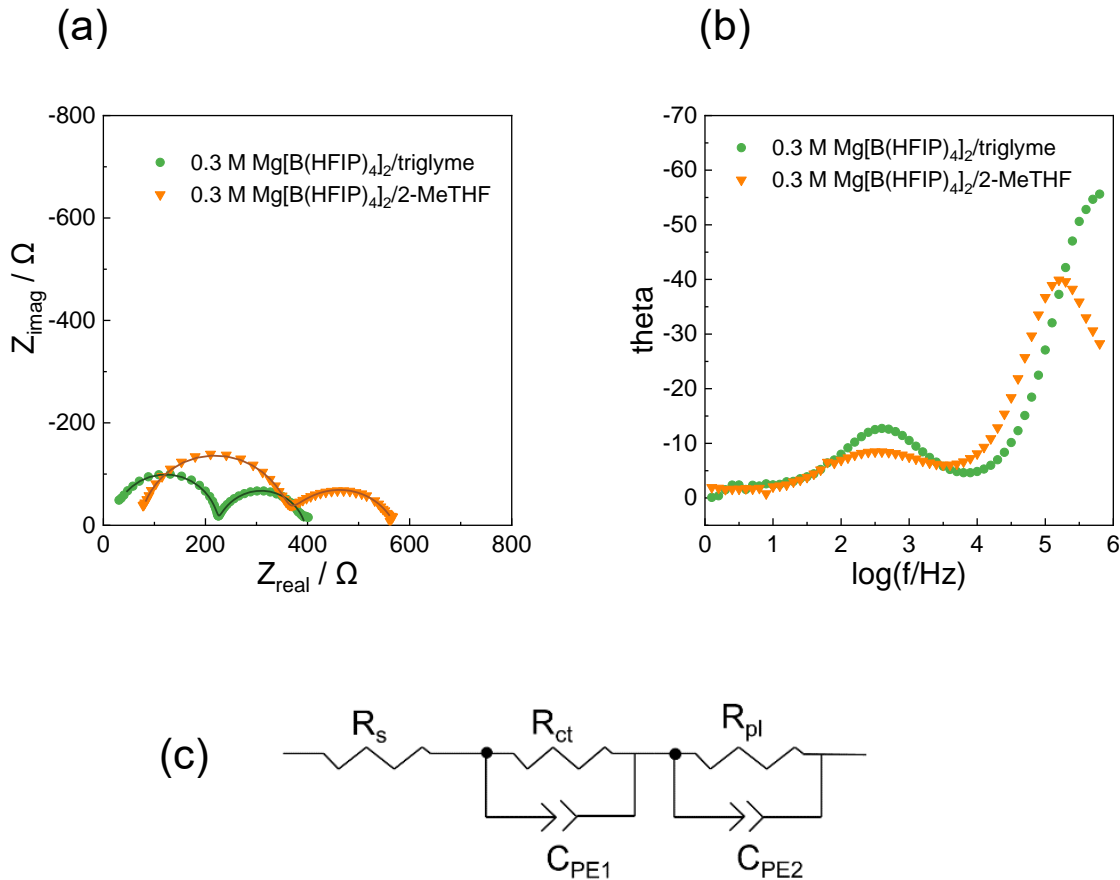


**Figure S12.** (a) Nyquist plots of deposited magnesium metal on Pt substrate in 0.3 M  $\text{Mg}[\text{B}(\text{HFIP})_4]_2/\text{triglyme}$ , and 0.3 M  $\text{Mg}[\text{B}(\text{HFIP})_4]_2/2\text{-MeTHF}$  electrolytes. Fitted impedance spectra shown in solid line. (b) Bode phase shift plot that donates the capacitive responses. (c) Equivalent circuit model, in which electrolyte solution resistance is  $R_s$ , charge transfer resistance is  $R_{\text{ct}}$ , constant phase element is  $C_{\text{PE1}}$ , passivation layer resistance is  $R_{\text{pl}}$  and constant phase element is  $C_{\text{PE2}}$ .

**Table S1.** The fitted parameter results of Figure 5.

Electrolyte	0.3 M Mg[B(HFIP) <sub>4</sub> ] <sub>2</sub> /triglyme	0.3 M Mg[B(HFIP) <sub>4</sub> ] <sub>2</sub> /2-MeTHF
R <sub>s</sub> / Ω	22.3	45.3
R <sub>ct</sub> / Ω	115.6	151.4
CPE	1.1 x 10 <sup>-8</sup>	5.3 x 10 <sup>-9</sup>
p	0.96	1.05
C / F	6.2 x 10 <sup>-9</sup>	1.0 x 10 <sup>-8</sup>
Time constant / s	7.9 x 10 <sup>-7</sup>	1.0 x 10 <sup>-6</sup>

**Table S2.** The fitted parameter results of Figure S12.

Electrolyte	0.3 M Mg[B(HFIP) <sub>4</sub> ] <sub>2</sub> /triglyme	0.3 M Mg[B(HFIP) <sub>4</sub> ] <sub>2</sub> /2-MeTHF
R <sub>s</sub> / Ω	18.25	71.4
R <sub>ct</sub> / Ω	205.8	287
CPE1	6.4 x 10 <sup>-9</sup>	1.3 x 10 <sup>-8</sup>
p1	0.97	0.95
C / F	4.2 x 10 <sup>-9</sup>	6.7 x 10 <sup>-9</sup>
Time constant / s	1.0 x 10 <sup>-6</sup>	2.0 x 10 <sup>-6</sup>
R <sub>pl</sub> / Ω	171.2	213.2
CPE2	1.1 x 10 <sup>-5</sup>	2.4 x 10 <sup>-5</sup>
p2	0.84	0.72
C / F	3.3 x 10 <sup>-6</sup>	3.1 x 10 <sup>-6</sup>
Time constant / s	6.3 x 10 <sup>-4</sup>	7.9 x 10 <sup>-4</sup>